

Tunnel magnetoresistance effect in magnetic tunnel junctions using Fermi-level-tuned epitaxial $\text{Fe}_2\text{Cr}_{1-x}\text{Co}_x\text{Si}$ Heusler alloy

Yu-Pu Wang,^{1,2,a)} Gu-Chang Han,² Hui Lu,¹ Jinjun Qiu,² Qi-Jia Yap,² and Kie-Leong Teo¹

¹Department of Electrical and Computer Engineering, National University of Singapore, 4 Engineering Drive 3, Singapore 117583

²Data Storage Institute, Agency for Science, Technology and Research (A*STAR), 5 Engineering Drive 1, Singapore 117608

(Presented 8 November 2013; received 15 September 2013; accepted 24 October 2013; published online 16 January 2014)

This paper reports a systematic investigation on the structural and magnetic properties of $\text{Fe}_2\text{Cr}_{1-x}\text{Co}_x\text{Si}$ Heusler alloys with various compositions of x by co-sputtering Fe_2CrSi and Fe_2CoSi targets and their applications in magnetic tunnel junctions (MTJs). $\text{Fe}_2\text{Cr}_{1-x}\text{Co}_x\text{Si}$ films of high crystalline quality have been epitaxially grown on MgO substrate using Cr as a buffer layer. The $L2_1$ phase can be obtained at $x = 0.3$ and 0.5 , while $B2$ phase for the rest compositions. A tunnel magnetoresistance (TMR) ratio of 19.3% at room temperature is achieved for MTJs using $\text{Fe}_2\text{Cr}_{0.3}\text{Co}_{0.7}\text{Si}$ as the bottom electrode with 350 °C post-annealing. This suggests that the Fermi level in $\text{Fe}_2\text{Cr}_{1-x}\text{Co}_x\text{Si}$ has been successfully tuned close to the center of band gap of minority spin with $x = 0.7$ and therefore better thermal stability and higher spin polarization are achieved in $\text{Fe}_2\text{Cr}_{0.3}\text{Co}_{0.7}\text{Si}$. The post-annealing effect for MTJs is also studied in details. The removal of the oxidized $\text{Fe}_2\text{Cr}_{0.3}\text{Co}_{0.7}\text{Si}$ at the interface with MgO barrier is found to be the key to improve the TMR ratio. When the thickness of the inserted Mg layer increases from 0.3 to 0.4 nm, the TMR ratio is greatly enhanced from 19.3% to 28%. © 2014 AIP Publishing LLC. [<http://dx.doi.org/10.1063/1.4862720>]

A significant number of experimental and theoretical works have been performed on half-metallic ferromagnets (HMFs) in the field of spintronics.¹ A number of full Heusler alloys have been predicted to be HMFs, which consists of four face-centered cubic sublattices in a chemical form of X_2YZ with $L2_1$ phase. These materials also assume $B2$ and $A2$ phase depending on the site-disordered state in which (Y, Z) and (X, Y, Z) are randomly substituted. The spin polarization of full Heusler alloy is believed to be sensitive to the site disorder.² The interests in Heusler alloys as spin polarized electron sources are aroused with the demonstration of large tunnel magnetoresistance (TMR) ratio at low temperature.³ However, the TMR ratio is dramatically degraded at room temperature (RT) due to the presence of quasi-particle states in the spin-down density of states (DOS) at the E_F and narrow energy separation between E_F and the conduction or valence band edge.⁴ The E_F tuning by alloying a fourth element to ternary Heusler alloy has been proposed to solve this problem and could enhance both the spin polarization and thermal stability by shifting E_F to the center of minority band gap.^{5,6}

Heusler alloy Fe_2CrSi (FCS) has been predicted to be a half metal with high spin polarization in $L2_1$ phase and relatively high Curie temperature (630 K).⁷ However, a low TMR of 8.1% at RT is obtained using FCS as the bottom electrode.⁸ The low TMR ratio is possibly because the E_F in FCS is close to the edge of minority bandgap. A recent theoretical study shows that E_F tuned $\text{Fe}_2\text{Cr}_{1-x}\text{Co}_x\text{Si}$ (FCCS) Heusler alloys are stable half-metallic ferromagnets and they are expected to have high TMR ratio.⁹

In this study, FCCS Heusler alloys with various compositions of x have been deposited and utilized in magnetic tunnel junctions (MTJs) as the bottom electrode. We have obtained $L2_1$ phase FCCS at $x = 0.3$ and 0.5 , and $B2$ phase for the rest compositions of x . The exchange bias (EB) with a shift of ~ 220 to 400 Oe is clearly observed for MTJs using FCCS as the bottom electrode. The post-annealing (T_a) effect is also studied in details. A TMR ratio of 19.3% at RT is obtained at $x = 0.7$ with $T_a = 350$ °C. Further enhancement of TMR ratio up to 28% (more than three times higher than that of FCS in Ref. 8) is achieved with an insertion of 0.4 nm thick of Mg layer between $\text{Fe}_2\text{Cr}_{0.3}\text{Co}_{0.7}\text{Si}$ bottom electrode and MgO barrier due to the removal of the oxidized interface.

The MTJs with a stacking structure of MgO (100)/Cr (40 nm)/FCCS (30 nm)/Mg (0.3 nm)/MgO (0.7 nm)/CoFe (3 nm)/IrMn (8 nm)/Ru (3 nm) were deposited by ultra-high vacuum magnetron sputtering system at ambient temperature with the base pressure of 10^{-7} Pa. The FCCS films with different x were prepared by a co-sputtering technique using Fe_2CrSi and Fe_2CoSi sputtering targets. The concentration was controlled by adjusting the input power of each sputtering target at a constant total deposition rate. The MgO barriers were grown by RF sputtering in a plasma oxidation chamber. An Mg layer of 0.3 nm thick was deposited onto the FCCS film prior to the deposition of MgO barrier to avoid the oxidation of FCCS. The *in-situ* thermal treatments were performed with temperature 600 °C for MgO substrate, 700 °C for Cr buffer layer to achieve flat surface, 400 °C for FCCS to promote chemical ordering, and 400 °C for MgO barrier layer to improve the crystalline and interface quality. The whole junctions were further post-annealed at

^{a)}Email: wangyupu@nus.edu.sg

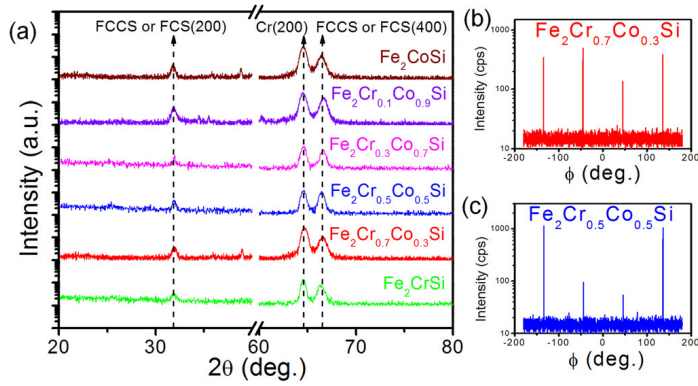


FIG. 1. (a) XRD patterns for MTJs using $\text{Fe}_2\text{Cr}_{1-x}\text{Co}_x\text{Si}$ ($x = 0, 0.3, 0.5, 0.7, 0.9$, and 1) as bottom electrodes. ϕ -scan of (111) orientation for (b) $\text{Fe}_2\text{Cr}_{0.7}\text{Co}_{0.3}\text{Si}$, and (c) $\text{Fe}_2\text{Cr}_{0.5}\text{Co}_{0.5}\text{Si}$.

temperature ranging from 235°C to 400°C for 1 h in high vacuum in the presence of an in-plane magnetic field of 1 Tesla.

Figure 1(a) shows the X-ray diffraction (XRD) patterns of MTJs using FCCS with Co composition x (0, 0.3, 0.5, 0.7, 0.9, and 1) as the bottom electrodes. Both (200) and (400) peaks for FCCS are observed, corresponding to $B2$ or $L2_1$ phase. One way to distinguish $B2$ and $L2_1$ phase is to perform a ϕ -scan where a diffraction peak from the (111) superlattice reflection can be observed only for $L2_1$ phase. As shown in Figs. 1(b) and 1(c), the (111) peak in the diffraction patterns is clearly observed, indicating the ordering of $L2_1$ phase for $\text{Fe}_2\text{Cr}_{0.7}\text{Co}_{0.3}\text{Si}$ and $\text{Fe}_2\text{Cr}_{0.5}\text{Co}_{0.5}\text{Si}$ films. On the other hand, the absence of (111) peak (not shown here) and the existence of (200) peak in Fig. 1(a) confirm the $B2$ phase for the rest of x composition. The ratio for the area under FCCS (400) peak over the area under FCCS (200) peak provides the degree of chemical ordering and the values are 5.33, 5.20, 5.57, 7.45, 4.07, and 5.06 for $x = 0, 0.3, 0.5, 0.7, 0.9$, and 1 , respectively. This suggests that the $\text{Fe}_2\text{Cr}_{0.3}\text{Co}_{0.7}\text{Si}$ has the highest chemical ordering. Furthermore, the full-width-at-half-maximum (FWHM) of (400) peak for FCCS for $x = 0, 0.3, 0.5, 0.7, 0.9$, and 1 are 0.74, 0.6, 0.57, 0.56, 0.71, and 0.71, respectively. This further indicates that $x = 0.7$ gives rise to the best crystalline structure. In addition, the lattice constants ranging from 5.6298 \AA to 5.6090 \AA for FCCS depending on the x composition can be obtained from the XRD results. We can see that there is no significant change in lattice parameters with x . This may be attributed to the small difference in atomic radius of Co and Cr. Our

estimated lattice constants are quite close to the theoretical values (5.679 \AA and 5.645 \AA for Fe_2CrSi and Fe_2CoSi , respectively).¹⁰ Hence, all FCCS films with different x are of high crystalline quality with $L2_1$ phase achieved at $x = 0.3$ and 0.5 while the rest belongs to $B2$ phase. In particular, $\text{Fe}_2\text{Cr}_{0.3}\text{Co}_{0.7}\text{Si}$ has the highest chemical ordering and best crystalline structure among all the samples.

Figure 2(a) shows the M - H loops of MTJs measured by alternating gradient magnetometer at RT. All samples show clear EB field (H_E) and H_E increases with x composition ($H_E = 220 \text{ Oe}$,⁸ 271 Oe , 279 Oe , 342 Oe , and 400 Oe for $x = 0, 0.3, 0.5, 0.7$, and 1 , respectively). The increment of H_E can be attributed to the highly ordered [111] orientation of CoFe/IrMn top electrode, which results from a better crystalline structure of the bottom electrode. Figure 2(b) presents the saturation magnetization (M_S) and coercivity (H_C) of FCCS as a function of x . The monotonous increment of M_S with x can be attributed to more valence electrons of Co than Cr. In addition, the solid line in Fig. 2(b) is a linear fitting of M_S , which follows the half-metallic Slater-Pauling rule, $M_S = Z - 24(\mu_B)$, where Z is the number of valence electrons.¹¹ This suggests that Heusler alloys FCCS are half-metallic candidates. The H_C values of FCCS with different x range from 4.3 Oe to 6.9 Oe , indicating a soft ferromagnetic nature.

The TMR effects were studied using Capres Current-In-Plane-Tunneling (CIPT) technique at RT on un-patterned samples.¹² The TMR ratio as a function of x is shown in Fig. 3(a). A TMR ratio of 19.3% at RT is achieved at $x = 0.7$ with $B2$ phase, rather than $x = 0.3$ and 0.5 with $L2_1$ phase. This suggests that the chemical ordering and the crystalline quality are more important to enhance the spin polarization rather than the phase formation. In addition, the E_F in $\text{Fe}_2\text{Cr}_{0.3}\text{Co}_{0.7}\text{Si}$ may have been tuned closer to the centre of band gap of minority spin, resulting in a better thermal stability. Hence, higher spin polarization with high TMR ratio is observed in $\text{Fe}_2\text{Cr}_{0.3}\text{Co}_{0.7}\text{Si}$. The T_a dependences of resistance-area product (RA) and TMR ratio of MTJs using $\text{Fe}_2\text{Cr}_{0.3}\text{Co}_{0.7}\text{Si}$ are shown in Fig. 3(b). The highest TMR ratio is achieved for the sample with $T_a = 350^\circ\text{C}$. The annealing of MTJs at an appropriate T_a improves not only the structural properties of the upper electrode but also the interfacial structural properties, leading to an enhancement of the TMR ratio. However, the TMR ratio drops dramatically at $T_a = 400^\circ\text{C}$. This is most likely due to the oxidation of $\text{Fe}_2\text{Cr}_{0.3}\text{Co}_{0.7}\text{Si}$ layer at the interface with the MgO barrier. The oxidized $\text{Fe}_2\text{Cr}_{0.3}\text{Co}_{0.7}\text{Si}$ surface may act as additional scattering centers for spin polarized tunnelling electrons, which would

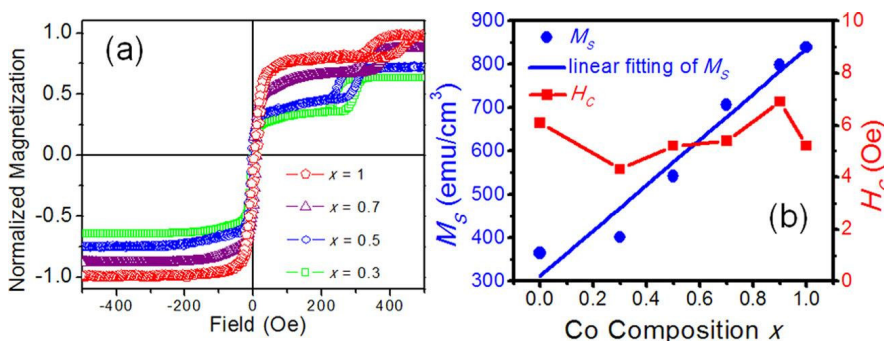


FIG. 2. (a) M - H loop of $\text{Fe}_2\text{Cr}_{1-x}\text{Co}_x\text{Si}$ ($x = 0.3, 0.5, 0.7$, and 1); (b) M_S and H_C of $\text{Fe}_2\text{Cr}_{1-x}\text{Co}_x\text{Si}$ as a function of Co composition x . The solid line is a linear fitting of M_S .

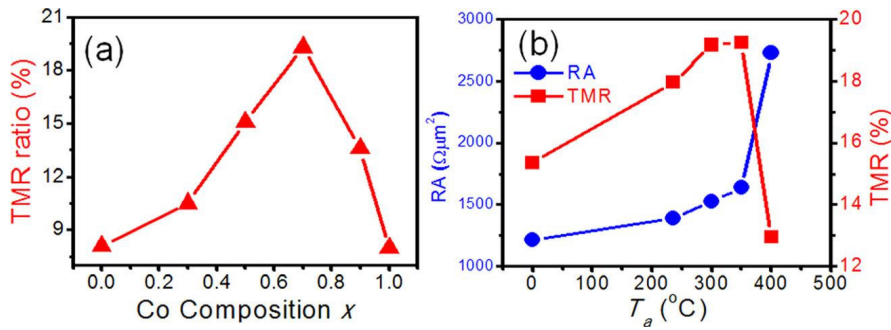


FIG. 3. (a) TMR ratio of MTJs using $\text{Fe}_2\text{Cr}_{1-x}\text{Co}_x\text{Si}$ ($x=0, 0.3, 0.5, 0.7, 0.9$, and 1) as a function of Co composition x ; (b) RA and TMR ratio of MTJs using $\text{Fe}_2\text{Cr}_{0.3}\text{Co}_{0.7}\text{Si}$ as a function of T_a .

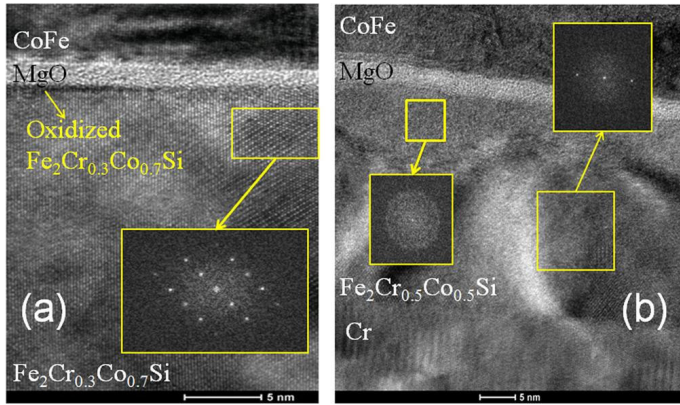


FIG. 4. (a) HRTEM of MTJs using (a) $\text{Fe}_2\text{Cr}_{0.3}\text{Co}_{0.7}\text{Si}$, or (b) $\text{Fe}_2\text{Cr}_{0.5}\text{Co}_{0.5}\text{Si}$ as bottom electrodes. The inset shows the FFT images.

suppress TMR ratio. The oxidation of $\text{Fe}_2\text{Cr}_{0.3}\text{Co}_{0.7}\text{Si}$ at the interface is further evidenced from the monotonically increasing of RA with T_a , especially the steep rise at $T_a = 400$ °C.

Figure 4 shows the cross-sectional high-resolution transmission electron microscopy (HRTEM) images of MTJs using $\text{Fe}_2\text{Cr}_{0.3}\text{Co}_{0.7}\text{Si}$ and $\text{Fe}_2\text{Cr}_{0.5}\text{Co}_{0.5}\text{Si}$ as bottom electrodes. The results show that the MTJ structures have good morphology with smooth and flat interface. All the layers are continuous without agglomerations. The fast Fourier transform images as shown in the inset of Figs. 4(a) and 4(b) confirm that $\text{Fe}_2\text{Cr}_{0.3}\text{Co}_{0.7}\text{Si}$ layer has better crystalline structure with higher ordering degree, as compared to $\text{Fe}_2\text{Cr}_{0.5}\text{Co}_{0.5}\text{Si}$, which boosts the TMR ratio. One problem is that $\text{Fe}_2\text{Cr}_{0.3}\text{Co}_{0.7}\text{Si}$ layer in some locations near the interface has been oxidized which are clearly revealed as a dark region in Fig. 4(a). In order to improve the TMR ratio, we increase the thickness of the inserted Mg layer from 0.3 to 0.4 nm to suppress the oxidation at the interface. As a result, the TMR ratio is enhanced to 28%, which is more than three times higher than that of FCS.⁸

In our study, the highest TMR ratio among $\text{Fe}_2\text{Cr}_{1-x}\text{Co}_x\text{Si}$ compounds is achieved at $x = 0.7$, while the theoretical calculation predicts that the highest TMR are expected at $x = 0.5$.⁹ From the DOS shown in Ref. 9, $\text{Fe}_2\text{Cr}_{0.25}\text{Co}_{0.75}\text{Si}$ is predicted to have slightly smaller spin polarization than $\text{Fe}_2\text{Cr}_{0.5}\text{Co}_{0.5}\text{Si}$ since the E_F lies at the valley of DOS of the majority spin. In our case, the spin polarization of $\text{Fe}_2\text{Cr}_{0.3}\text{Co}_{0.7}\text{Si}$ is expected to increase significantly since with a slightly less Co-doping will move the E_F closer to the center of energy band gap of minority

spin and out of the valley of DOS of majority spin. Thus, $\text{Fe}_2\text{Cr}_{0.3}\text{Co}_{0.7}\text{Si}$ could have the highest spin polarization among FCCS samples with thermal stability leading to high TMR ratio. This is consistent with our experimental results. Furthermore, the ferromagnet/insulator interface plays a critical role in the enhancement of the TMR ratio. The removal of interface defects would effectively increase the TMR ratio. In our study, an additional 0.1 nm thick of Mg layer insertion has efficiently prevented the oxidation and significantly improved the TMR ratio. However, there could be Mg residual in some locations along the interface and it is hard to control the exact Mg thickness for a perfect interface at which there is neither metallic Mg residual nor oxidized bottom electrode. Therefore, TMR ratio obtained is still much lower than the expected value. In addition, the TMR ratio could be further enhanced if high chemical ordering and crystalline quality with $L2_1$ phase $\text{Fe}_2\text{Cr}_{0.3}\text{Co}_{0.7}\text{Si}$ structure could be achieved.

In summary, we have epitaxially grown and studied the structural and magnetic properties of FCCS Heusler alloys with various compositions of x . The $L2_1$ phase are obtained for $x = 0.3$ and 0.5 , while $B2$ phase are observed for the rest of x compositions. The highest TMR ratio is achieved as 19.3% at RT for MTJs using $\text{Fe}_2\text{Cr}_{0.3}\text{Co}_{0.7}\text{Si}$ as the bottom electrode. This suggests that the E_F in $\text{Fe}_2\text{Cr}_{0.3}\text{Co}_{0.7}\text{Si}$ has been tuned close to the center of band gap of minority spin, resulting in a better thermal stability and higher spin polarization. In addition, the removal of the oxidized $\text{Fe}_2\text{Cr}_{0.3}\text{Co}_{0.7}\text{Si}$ at the interface by MgO barrier layer is the key to improve the TMR ratio. Our results show that with a 0.4 nm thick of Mg layer insertion, the TMR ratio can be increased to 28%.

This work was supported by Singapore Agency for Science, Technology and Research (A*STAR), under Grant No. 092-151-0087.

¹R. A. de Groot *et al.*, *Phys. Rev. Lett.* **50**, 2024 (1983).

²Y. Miura *et al.*, *Phys. Rev. B* **69**, 144413 (2004).

³Y. Sakuraba *et al.*, *Appl. Phys. Lett.* **88**, 192508 (2006).

⁴L. Chioncel *et al.*, *Phys. Rev. Lett.* **96**, 137203 (2006).

⁵I. Galanakis, *J. Phys. Condens. Matter* **16**, 3089 (2004).

⁶G. H. Fecher and C. Felser, *J. Phys. D: Appl. Phys.* **40**, 1582 (2007).

⁷S. Yoshimura *et al.*, *J. Appl. Phys.* **103**, 07D716 (2008).

⁸Y. P. Wang *et al.*, *J. Appl. Phys.* **114**, 013910 (2013).

⁹Y. Du *et al.*, *J. Magn. Magn. Mater.* **335**, 101 (2013).

¹⁰H. Z. Luo *et al.*, *J. Phys. D: Appl. Phys.* **40**, 7121 (2007).

¹¹I. Galanakis *et al.*, *Phys. Rev. B* **66**, 174429 (2002).

¹²D. C. Worledge and P. L. Trouilloun, *Appl. Phys. Lett.* **83**, 84 (2003).